

Serveur Académique Lausannois SERVAL [serval.unil.ch](http://serval.unil.ch)

## Author Manuscript

Faculty of Biology and Medicine Publication

This paper has been peer-reviewed but does not include the final publisher proof-corrections or journal pagination.

Published in final edited form as:

**Title:** Differential effects of glutamate transporter inhibitors on the global electrophysiological response of astrocytes to neuronal stimulation.

**Authors:** Bernardinelli Y, Chatton JY

**Journal:** Brain research

**Year:** 2008 Nov 13

**Issue:** 1240

**Pages:** 47-53

**DOI:** 10.1016/j.brainres.2008.09.014

In the absence of a copyright statement, users should assume that standard copyright protection applies, unless the article contains an explicit statement to the contrary. In case of doubt, contact the journal publisher to verify the copyright status of an article.

# Differential effects of glutamate transporter inhibitors on the global electrophysiological response of astrocytes to neuronal stimulation.

by

Yann Bernardinelli<sup>1,§</sup> and Jean-Yves Chatton<sup>1,2,3</sup>

<sup>1</sup>Department of Physiology, <sup>2</sup>Department of Cell Biology and Morphology, and <sup>3</sup>Cellular Imaging Facility, University of Lausanne, Switzerland

Number of pages: 17

Number of figures: 3

Corresponding author:

Dr. Jean-Yves Chatton, PD MER  
Department of Cell Biology and Morphology  
Rue du Bugnon 9  
CH-1005 Lausanne  
Switzerland  
Tel: +41-21-692-5106  
Fax: +41-21-692-5105  
E-mail: jean-yves.chatton@unil.ch

## Footnote

§ Present address: Center for Research in Neuroscience, Research Institute of the McGill University Health Centre, Montreal, Quebec, Canada. Supported by fellowship #PBLAB-118155 from the Swiss National Science Foundation

Abbreviations: GLT-1, glutamate transporter 1; GLAST, glutamate-aspartate transporter; TBOA, DL-*threo*- $\beta$ -benzyloxyaspartate; DHK, dihydrokainate; TTX, tetrodotoxin; Kir, inwardly rectifying K<sup>+</sup> channels; I-V, current-voltage; I<sub>Trsp</sub>, glutamate transporter current; I<sub>Tail</sub>, persistent inward K<sup>+</sup> current; Ba<sup>2+</sup>, barium

## Abstract

Astrocytes are responsible for regulating extracellular levels of glutamate and potassium during neuronal activity. Glutamate clearance is handled by glutamate transporter subtypes glutamate transporter 1 and glutamate-aspartate transporter in astrocytes. DL-*threo*- $\beta$ -benzyloxyaspartate (TBOA) and dihydrokainate (DHK) are extensively used as inhibitors of glial glutamate transport activity. Using whole-cell recordings, we characterized the effects of both transporter inhibitors on afferent-evoked astrocyte currents in acute cortical slices of 3-week-old rats. When neuronal afferents were stimulated, passive astrocytes responded by a rapid inward current followed by a persistent tail current. The first current corresponded to a glutamate transporter current. This current was inhibited by both inhibitors and by tetrodotoxin. The tail current is an inward potassium current as it was blocked by barium. Besides inhibiting transporter currents, TBOA strongly enhanced the tail current. This effect was barium-sensitive and might be due to a rise in extracellular potassium level and increased glial potassium uptake. Unlike TBOA, DHK did not enhance the tail current but rather inhibited it. This result suggests that, in addition to inhibiting glutamate transport, DHK prevents astrocyte potassium uptake, possibly by blockade of inward-rectifier channels. This study revealed that, in brain slices, glutamate transporter inhibitors exert complex effects that cannot be attributed solely to glutamate transport inhibition.

Section: 3. Neurophysiology, Neuropharmacology and other forms of Intercellular Communication.

Keywords: astrocytes; DL-*threo*- $\beta$ -benzyloxyaspartate, dihydrokainate; glutamate transport; potassium buffering, cortical slice

## 1. Introduction

Neuronal activity at glutamatergic synapses leads to substantial glutamate release and  $K^+$  efflux in the extracellular space. The clearance of both glutamate and  $K^+$  are crucial functions of astrocytes in the nervous system. By rapidly taking up extracellular glutamate, astroglial cells protect neurons from the excitotoxic buildup of glutamate and ensure the fidelity of glutamatergic transmission at high frequency (Danbolt, 2001). For that purpose, astrocytes are equipped with efficient glutamate transporters that surround the synaptic cleft and use the electrochemical gradient of  $Na^+$  to take up glutamate. Among the five subtypes that have been identified so far, both glutamate-aspartate transporter (GLAST) and glutamate transporter 1 (GLT-1) are expressed by glial cells and account for most of the glutamate uptake activity in the CNS (Danbolt, 2001). In parallel to the glutamate clearance, glial cells express inwardly rectifying  $K^+$  (Kir) channels to enable  $K^+$  regulation. Within the seven described Kir families, the Kir4.1 subtype is almost exclusively expressed by glia in the CNS (Higashi et al., 2001; Butt and Kalsi, 2006).

Inhibitors of glutamate transporters are inevitably crucial tools for elucidating the physiological roles of these transporters in detail. Several compounds have traditionally been used to inhibit glutamate transport, such as *threo*- $\beta$ -hydroxyaspartate and *trans*-pyrrolidine-2,4-dicarboxylic acid, both of which are transported competitive inhibitors without subtype selectivity (Chatton et al., 2001). More recently, the compound DL-*threo*- $\beta$ -benzyloxyaspartate (TBOA) has been introduced and then widely used as a non-transported competitive inhibitor of glutamate transporters (Shimamoto et al., 1998). TBOA, however, has a similar affinity for all subtypes of glutamate transporters (Shimamoto et al., 2004). The compound dihydrokainate (DHK) has been early on identified as a GLT-1 selective inhibitor. Most studies on the effects of transport inhibitors have been performed on primary cultured cells (e.g. Chatton et al., 2001) or have focused on the effects of these transporter inhibitors on expression systems such as COS-1 cells or mRNA-injected *Xenopus* oocytes (Shimamoto et al., 1998; Shimamoto et al., 2004). Despite the lack of data on their effects in experimental preparations where cellular interactions are preserved, both TBOA and DHK are now extensively used to block glial glutamate transport in studies investigating neuron-glia interactions (see Volterra and Meldolesi, 2005 for an extensive review on neuron-glia interactions). Moreover, since glial glutamate transport dysfunction has been proposed to have a central role in mood disorder (Sanacora et al., 2003), glutamate transporter inhibitors start to be used as novel treatment directions for these pathologies (Lee et al., 2007).

The evoked whole-cell events recorded from astrocytes in acute slices are characterized by a first short-lived inward current, previously identified as reflecting glutamate transporter activity (Bergles and Jahr, 1997). This initial current is followed by a low amplitude sustained inward current described in the literature as being an inward  $K^+$  current consecutive to the increased extracellular  $K^+$  caused by neuronal activity (Bergles and Jahr, 1997; De Saint Jan and Westbrook, 2005). This  $K^+$  influx, which is mediated by Kir channels (Newman, 1993), participates to the astrocytic  $K^+$  buffering processes (Walz, 2000; Wallraff et al., 2006).

In the presents study, we evaluated the effects of the two widely used inhibitors of glutamate transporters, TBOA and DHK, on glutamate transporter currents and potassium uptake in astrocytes in brain slices. We found that they have different effects on the overall astrocytic response.

## 2. Results

Two main types of astroglial cells coexist in the developing rat brain (Steinhauser et al., 1994). The so-called passive astrocytes are characterized by their expression of glutamate transporters, as seen by the transporter currents recorded following neuronal afferent stimulation (Zhou et al., 2006). Complex or rectifying cells are characterized by the absence of significant glutamate transporter activity, with however, expression of ionotropic glutamate receptors (Matthias et al., 2003; Wallraff et al., 2004). Here, in slices of the somato-sensory cortex acutely isolated from 15- to 21-days old rats, the presence of these two types of astrocytes was also observed. Slices were visualized on an upright microscope equipped with infrared–differential interference contrast. Astroglial cells were selected in layer I by their small soma size ( $<10\mu\text{m}$ ), and then recorded in whole-cell configuration. Their complex morphology was verified by tridimensional reconstruction from confocal fluorescent images of the cell filled with Lucifer Yellow (LY,  $500\mu\text{M}$ ) through the patch pipette (Fig. 1A). By doing so, 71% of the patched cells were found to be passive astrocytes. They were identified by their linear current-voltage (I-V) relationship (Fig. 1B), the lack of action potentials, their very negative resting potential ( $-81.0 \pm 1.1\text{mV}$ ), their high membrane capacitance ( $348 \pm 172\text{pF}$ ) and the very low membrane resistance ( $15.0 \pm 4.5\text{M}\Omega$ ). Complex astrocytes were recognized by a less negative potential ( $-77.1 \pm 1.9\text{mV}$ ), a higher membrane resistance ( $177 \pm 37\text{M}\Omega$ ), a lower membrane capacitance ( $69.8 \pm 11.5\text{pF}$ ) and a non-linear I-V curve (Fig. 1C). The present study focuses on passive astrocytes.

When neuronal afferents were electrically stimulated, passive astrocytes displayed a rapid inward current followed by a persistent inward current (Fig. 2A). The rapid current was inhibited by glutamate transport inhibitors TBOA (Figs. 2A and C) and DHK (*see below* Fig. 3A) and displayed a time to peak of  $12.7 \pm 1.2\text{msec}$  with a maximum amplitude of  $-111.5 \pm 15.9\text{ pA}$  ( $n=10$ ). Moreover, this current was neuronal activity-dependent as its amplitude was proportional with the intensity of the applied stimulation and disappeared in the presence of TTX ( $1\mu\text{M}$ , not shown). These data suggest that this current corresponds to a glutamate transporter current ( $I_{\text{Trsp}}$ ) as described previously (Bergles and Jahr, 1997).  $I_{\text{Trsp}}$  was followed by a persistent “tail current” ( $I_{\text{Tail}}$ ). This current was an inward current of low amplitude that monotonically reached baseline levels after  $8.0 \pm 1.0$  seconds (Time to baseline,  $n=10$  exp, Fig. 2A). Whereas TBOA applied alone almost entirely inhibited  $I_{\text{Trsp}}$  within  $4 \pm 1$  minutes of application, it dramatically changed the  $I_{\text{Tail}}$  time course and amplitude (Figs. 2A and B). Under TBOA,  $I_{\text{tail}}$  displayed a 3-fold enhancement of its maximum amplitude (Fig. 2C), and a 2.5 fold increased of the time needed for return to baseline (Fig. 2C).

Astrocytes are generally considered to have a very negative (-70-80mV) and stable resting membrane potential. We nevertheless tested whether in these situations membrane potential was altered during evoked neuronal activity, and analyzed these astrocytic responses in current-clamp mode. We observed that cells responded to afferent stimulations by small and transient depolarizations of ~3mV that were inhibited by TBOA (Fig. 2D), therefore assigned to transporter-activity ( $V_{Trsp}$ ). Following this transient, a persistent increased potential lasting several seconds was observed. Interestingly, and consistent with voltage-clamp measurements, in the presence of TBOA, this persistent increased membrane potential ( $V_{Tail}$ ) showed a >2-fold increase (Figs. 2D and E). These results are consistent with the notion that TBOA leads to an enhancement of the extracellular  $K^+$  concentration during the firing of presynaptic afferents.

In order to verify whether  $I_{Tail}$  has indeed a  $K^+$  origin, as suggested by others (Bergles and Jahr, 1997; De Saint Jan and Westbrook, 2005; Meeks and Mennerick, 2007), we applied 200 $\mu$ M  $Ba^{2+}$  in the bath (Fig. 3A). At this concentration, which effectively blocks Kir channels of glial cells (Newman, 1993),  $Ba^{2+}$  inhibited the majority of  $I_{Tail}$ , and had a slight but non-significant inhibitory effect on  $I_{Trsp}$ , possibly reflecting a modest effect on neuronal transmitter release. Moreover, when  $Ba^{2+}$  and TBOA were applied in combination, both  $I_{Trsp}$  and  $I_{Tail}$  essentially disappeared (Fig. 3A). Accordingly, the time to baseline in the presence of  $Ba^{2+}$  was markedly reduced (Fig. 3A). Thus, the massive enhancement of  $I_{Tail}$  caused by TBOA was absent in the presence of  $Ba^{2+}$ , indicating that this current had effectively a  $K^+$  origin.

If the  $I_{tail}$  enhancement by TBOA was due to astrocytic  $K^+$  influx through Kir conductances, other glutamate transporter inhibitors would be expected to have similar effects on  $I_{Tail}$ . We therefore tested DHK, another non-transported glutamate transporter inhibitor. As expected, Fig. 3B shows that DHK (100-300 $\mu$ M) inhibited  $I_{Trsp}$  by 50-70%. The maximal inhibition was of the same magnitude as with TBOA. In contrast to TBOA, not only did DHK fail to enhance  $I_{Tail}$ , but it actually prevented its manifestation. Thus, DHK application led to the same response pattern as the addition of TBOA and  $Ba^{2+}$  together. Moreover, in the presence of DHK, the whole-cell current voltage-relationship curve of the cell measured from the baseline (e.g. in non-evoked astrocytic currents condition), showed a significantly decreased slope indicative of an increased input resistance (Fig. 3C), and a shift of the membrane potential to more depolarized values, consistent with the notion that DHK leads to a closure of conductances. All together these results could indicate that, in addition to inhibiting glutamate transport, DHK also prevents astrocyte  $K^+$  uptake.

### 3. Discussion

The effects of inhibition of glial glutamate transport in the intact tissue have been most often discussed in terms of glutamate spill-over from the synaptic cleft and its action on neuronal extrasynaptic receptors (Volterra and Meldolesi, 2005). The present study demonstrates that glutamate transporter inhibitors exert different effects on the astrocytic  $K^+$  response to neuronal stimulation, which are not attributable solely to glutamate transport inhibition.

In agreement with previous reports, TBOA efficiently inhibited the first, transporter-mediated, component. However, a large inward current was then observed that lasted for several seconds. The onset of this current corresponded to that of the tail current attributed to  $K^+$  uptake; however its amplitude and duration were up to 3-fold increased. Because this enhanced current was abolished by barium, it could be attributed to an enhancement of astrocytic  $K^+$  uptake. It has to be borne in mind that inhibiting glutamate transport in the intact tissue causes the accumulation of extracellular glutamate which strongly enhances neuronal excitability, even leading to epileptiform activity (Campbell and Hablitz, 2004). The enhancement of activity is therefore most likely accompanied by substantial  $K^+$  accumulation in the extracellular space.

This observation is possibly similar to what was reported in cerebellar slices, where a slow inward current was observed in Bergmann glial (Bellamy and Ogden, 2005). This current was enhanced by TBOA and was proposed to be caused by a paracrine messenger released from neurons to activate a G-protein coupled receptor in Bergman glia eventually opening some conductance. It should be noted that only a couple of studies have documented the TBOA potentiation of the  $K^+$  current (Bellamy and Ogden, 2005; De Saint Jan and Westbrook, 2005), probably because most of other studies have focused on the transporter component.

During the course of this study, we reasoned that a similar pattern of responses should be observed in the presence of the other widely used non-transported glutamate transporter inhibitor DHK. Whereas TBOA inhibits all transporter subtypes (Shimamoto et al., 2004), DHK acts selectively on the GLT-1 subtype. In the same experimental conditions, both DHK and TBOA inhibited the transporter current. Unexpectedly, DHK not only failed to enhance the tail current, but it completely prevented its manifestation. Potency of DHK at GLT-1 is relatively low with an  $IC_{50}$  of  $56\mu M$  (Shimamoto et al., 2004) and DHK displays binding at kainate receptors at concentrations similar to those required for GLT1 inhibition, as well as weak antagonistic effects of NMDA receptors (Selkirk et al., 2005). The present study unveiled a new aspect of DHK effects *in situ*, being that, in addition to inhibiting glutamate transport, DHK prevented astrocyte  $K^+$  uptake, possibly by blockade of inward-rectifier channels.



Because of the different selectivity of TBOA and DHK for transporter subtypes, one could argue the apparent different effects of these inhibitors arise from the subtypes they target. Here, TBOA and DHK showed similar maximal inhibitory level of  $I_{trsp}$ , consistent with the fact that between postnatal days 15 and 21, both GLT-1 and GLAST are expressed by rat astrocytes. In consequence, the observed difference on the  $K^+$  current should not be only attributed to a different inhibitory level of the two compounds.

In conclusion, when using glutamate transporter inhibitors to study glutamate transport *in situ*, complex and indirect effects will impinge on the functions not only of astrocytes but also of neurons. This study revealed that glutamate transporter inhibitors TBOA and DHK exert strikingly different effects on glial responses to neuronal activity.

## 4. Experimental Procedure

### 4.1. Acute cortical slice preparation

Experiments were performed on 350µm thick slices of the somatosensory cortex, identified as described previously (Lalo and Kostyuk, 1998; Pankratov et al., 2002). Briefly, after isoflurane anesthesia, Sprague-Dawley rats were decapitated. Coronal slices were cut in slice cutting solution (SCS) using a vibrating slicer (VT 1000S, Leica, Germany) and kept in artificial cerebrospinal fluid (ACSF) at room temperature. The ACSF solution contained (in mM): NaCl 126, KCl 2.5, NaHCO<sub>3</sub> 26, CaCl<sub>2</sub> 2, MgCl<sub>2</sub> 2, NaH<sub>2</sub>PO<sub>4</sub> 1.25, glucose 10, bubbled with 5% CO<sub>2</sub>/95% oxygen. The SCS solution contained (in mM): KCl 2.5, NaHCO<sub>3</sub> 25, CaCl<sub>2</sub> 0.5, MgSO<sub>4</sub> 7, NaH<sub>2</sub>PO<sub>4</sub> 1.25, glucose 25, choline chloride 110, Na-L-ascorbate 11.6, Na-pyruvate 3.1, and was bubbled with 5% CO<sub>2</sub>/95% oxygen. Threo-β-benzyloxyaspartate (TBOA) and dihydrokainic acid (DHK) were from Tocris-Anawa Trading (Zürich). Lucifer Yellow was from Molecular Probes. All other compounds were from Sigma.

### 4.2. Whole-cell electrophysiological recordings and imaging

Whole-cell voltage- and current-clamp recordings were made with borosilicate glass pipettes with a resistance of 5.5-8 MΩ. In voltage-clamp mode, the clamp potential was set at the astrocyte resting potential. Recordings were made with an Axopatch 200 amplifier (Axon Instruments). Current were filtered at 2 kHz. Data were acquired with a Digidata 1322A (Axon), controlled with Pclamp 9 software and analyzed with Clampfit software (Axon). Experiments with unstable holding current and/or access resistance were discarded. A period of 5 min was routinely allowed after establishment of the whole-cell configuration. The patch-clamp intracellular solution contained (in mM): K-gluconate 124, NaCl 6, KCl 6, MgCl<sub>2</sub> 3, EGTA 1, CaCl<sub>2</sub> 0.5, HEPES 10, glutathione 2, Mg-ATP 3, Na<sub>3</sub>-GTP 0.3, pH 7.3 (with KOH).

Excitatory afferents were stimulated by applying a single depolarization square pulse (0.25msec) generated by a Grass S8800 stimulator (Astro Med, West Warwick, RI, USA) through a concentric bipolar tungsten electrode (Micro Probe, Gaithersburg, MD, USA). The stimulating electrode was positioned at least at 150µm from the patch pipette in higher cortical layers. The stimulus strength was adjusted to produce astrocytic responses that were ~80% of the maximum. Afferent stimulations were generated and recorded every minute during the entire experiments. Drugs were applied after 3 control pulses by bath superfusion. Confocal imaging was performed using a confocal microscope (LSM 510 Meta). Three dimensional images were reconstructed using the software Imaris (Bitplane, Zurich, Switzerland).

#### 4.3. Data analysis

For a given experiment, the mean of the three control responses was calculated and used to normalize the response expressed in percentage. Data are means  $\pm$  SEM and are represented as percentage of the control current or voltage amplitude. A paired student t-test was performed to assess the statistical significance (\*,  $P < 0.05$ ; \*\*,  $P \leq 0.01$ ; \*\*\*,  $P < 0.001$ ). The number n represents independent experiments performed on different brain slices.

## **Acknowledgments**

We gratefully acknowledge Charles Bourque for the careful reading of the manuscript, Hubert Fiumelli and Christophe Lamy for fruitful discussions, and Khaleel Bhaukaurally, for his technical advice on brain slices. We thank Yannick Krempp and the CIF for the 3D reconstructions.. Supported by grants #3100A0-108395 and #3100A0-119827 from the Swiss National Science Foundation to JY Chatton.

## References

- Bellamy, T.C., Ogden, D., 2005. Short-term plasticity of Bergmann glial cell extrasynaptic currents during parallel fiber stimulation in rat cerebellum. *Glia*. 52, 325-335.
- Bergles, D.E., Jahr, C.E., 1997. Synaptic activation of glutamate transporters in hippocampal astrocytes. *Neuron*. 19, 1297-1308.
- Butt, A.M., Kalsi, A., 2006. Inwardly rectifying potassium channels (Kir) in central nervous system glia: a special role for Kir4.1 in glial functions. *J Cell Mol Med*. 10, 33-44.
- Campbell, S.L., Hablitz, J.J., 2004. Glutamate transporters regulate excitability in local networks in rat neocortex. *Neuroscience*. 127, 625-635.
- Chatton, J.-Y., Shimamoto, K., Magistretti, P.J., 2001. Effects of glial glutamate transporter inhibitors on intracellular Na<sup>+</sup> in mouse astrocytes. *Brain Research*. 893, 46-52.
- Danbolt, N.C., 2001. Glutamate uptake. *Prog. Neurobiol.*, 65, 1-105.
- De Saint Jan, D., Westbrook, G.L., 2005. Detecting activity in olfactory bulb glomeruli with astrocyte recording. *J Neurosci*. 25, 2917-2924.
- Higashi, K., Fujita, A., Inanobe, A., Tanemoto, M., Doi, K., Kubo, T., Kurachi, Y., 2001. An inwardly rectifying K(+) channel, Kir4.1, expressed in astrocytes surrounds synapses and blood vessels in brain. *Am J Physiol Cell Physiol*. 281, C922-931.
- Lalo, U., Kostyuk, P., 1998. Developmental changes in purinergic calcium signalling in rat neocortical neurones. *Brain Res Dev Brain Res*. 111, 43-50.
- Lee, Y., Gaskins, D., Anand, A., Shekhar, A., 2007. Glia mechanisms in mood regulation: a novel model of mood disorders. *Psychopharmacology (Berl)*. 191, 55-65.
- Matthias, K., Kirchhoff, F., Seifert, G., Huttmann, K., Matyash, M., Kettenmann, H., Steinhauser, C., 2003. Segregated expression of AMPA-type glutamate receptors and glutamate transporters defines distinct astrocyte populations in the mouse hippocampus. *J Neurosci*. 23, 1750-1758.
- Meeks, J.P., Mennerick, S., 2007. Astrocyte membrane responses and potassium accumulation during neuronal activity. *Hippocampus*. 17, 1100-1108.
- Newman, E.A., 1993. Inward-rectifying potassium channels in retinal glial (Muller) cells. *J Neurosci*. 13, 3333-3345.

- Pankratov, Y., Lalo, U., Krishtal, O., Verkhratsky, A., 2002. Ionotropic P2X purinoreceptors mediate synaptic transmission in rat pyramidal neurones of layer II/III of somato-sensory cortex. *J Physiol.* 542, 529-536.
- Sanacora, G., Rothman, D.L., Mason, G., Krystal, J.H., 2003. Clinical studies implementing glutamate neurotransmission in mood disorders. *Ann N Y Acad Sci.* 1003, 292-308.
- Selkirk, J.V., Nottebaum, L.M., Vana, A.M., Verge, G.M., Mackay, K.B., Stiefel, T.H., Naeve, G.S., Pomeroy, J.E., Petroski, R.E., Moyer, J., Dunlop, J., Foster, A.C., 2005. Role of the GLT-1 subtype of glutamate transporter in glutamate homeostasis: the GLT-1-preferring inhibitor WAY-855 produces marginal neurotoxicity in the rat hippocampus. *Eur J Neurosci.* 21, 3217-3228.
- Shimamoto, K., Lebrun, B., Yasuda-Kamatani, Y., Sakaitani, M., Shigeri, Y., Yumoto, N., Nakajima, T., 1998. DL-threo-beta-benzyloxyaspartate, a potent blocker of excitatory amino acid transporters. *Mol Pharmacol.* 53, 195-201.
- Shimamoto, K., Sakai, R., Takaoka, K., Yumoto, N., Nakajima, T., Amara, S.G., Shigeri, Y., 2004. Characterization of novel L-threo-beta-benzyloxyaspartate derivatives, potent blockers of the glutamate transporters. *Mol Pharmacol.* 65, 1008-1015.
- Steinhauser, C., Jabs, R., Kettenmann, H., 1994. Properties of GABA and glutamate responses in identified glial cells of the mouse hippocampal slice. *Hippocampus.* 4, 19-35.
- Volterra, A., Meldolesi, J., 2005. Astrocytes, from brain glue to communication elements: the revolution continues. *Nat Rev Neurosci.* 6, 626-640.
- Wallraff, A., Kohling, R., Heinemann, U., Theis, M., Willecke, K., Steinhauser, C., 2006. The impact of astrocytic gap junctional coupling on potassium buffering in the hippocampus. *J Neurosci.* 26, 5438-5447.
- Wallraff, A., Odermatt, B., Willecke, K., Steinhauser, C., 2004. Distinct types of astroglial cells in the hippocampus differ in gap junction coupling. *Glia.* 48, 36-43.
- Walz, W., 2000. Role of astrocytes in the clearance of excess extracellular potassium. *Neurochem Int.* 36, 291-300.
- Zhou, M., Schools, G.P., Kimelberg, H.K., 2006. Development of GLAST(+) astrocytes and NG2(+) glia in rat hippocampus CA1: mature astrocytes are electrophysiologically passive. *J Neurophysiol.* 95, 134-143.

## Figure legends

Fig. 1 - *Electrophysiological identification of astrocytes*. (A). Tridimensional reconstruction from confocal fluorescent images of an astroglial cell filled with LY (major tick = 10 $\mu$ m). (B) Representative whole-cell current response of a passive astrocyte to 20mV steps of voltage (-160mV to 20mV). The cell was clamped at -80mV under resting condition. (C) Representative current response of a complex glial cell to voltage steps. I-V curve demonstrates outward rectification of the peak currents.

Fig. 2 - *Effect of TBOA on the voltage and current astrocytic response*. (A) Whole-cell voltage clamp response of passive astrocyte to brief neuronal stimulation. Dotted lines indicate the baseline current level. Bath application of TBOA (100 $\mu$ M) rapidly inhibited  $I_{Trsp}$  and increased  $I_{Tail}$ . (B) Timecourse of TBOA effects on  $I_{Tail}$  and  $I_{Trsp}$ . Number of independent experiments for each time point is indicated in the graph. (C) The graph shows the effect of TBOA on  $I_{Tail}$ ,  $I_{Trsp}$  and the time-to-baseline (n=8). (D) Whole-cell current clamp response. A depolarization transient accompanied  $I_{Trsp}$  and a slight persistent depolarization was observed during  $I_{Tail}$  (lower trace). The fast depolarization was completely abolished by TBOA, whereas the persistent depolarization was enhanced. (E) Bar graph showing means of voltage amplitude following afferent stimulation in control condition (white bars) and in the presence of TBOA (black bars) for both fast ( $V_{Trsp}$ ) and persistent ( $V_{Tail}$ ) voltage components (n=5).

Fig. 3.- *DHK prevents Barium-sensitive evoked current and closes conductances*. (A) In the presence of  $Ba^{2+}$ , most of  $I_{Tail}$  disappeared (middle trace), leaving  $I_{Trsp}$  that could be blocked by the glutamate transporter inhibitor TBOA (bottom trace). Bath application of  $Ba^{2+}$  blocked 76% of the evoked  $I_{Tail}$  amplitude and reduced the Time-to-Baseline (*not shown*) by 85%.  $I_{Trsp}$  was not significantly inhibited by  $Ba^{2+}$  (n=5). (B) Application of DHK inhibited up to 73% of  $I_{Trsp}$  as did TBOA; however, to achieve this level of inhibition, DHK required twice as long incubation time ( $8.1 \pm 2.1$  min, n=7). In the presence of DHK,  $I_{Tail}$  was strongly impaired compared to the control. Bar graph showing that DHK reduced  $I_{Tail}$  amplitude by up to 62% and the time-to-baseline by 48%. Data are shown for a DHK incubation time of 4 min (white bars) and for a time corresponding to the maximal  $I_{Trsp}$  inhibition (black bars). (C) I-V-curve before (open circles) and during (black diamonds) DHK superfusion (n=4) showing a decreased slope (increased input resistance) and change of equilibrium potential towards more positive values.

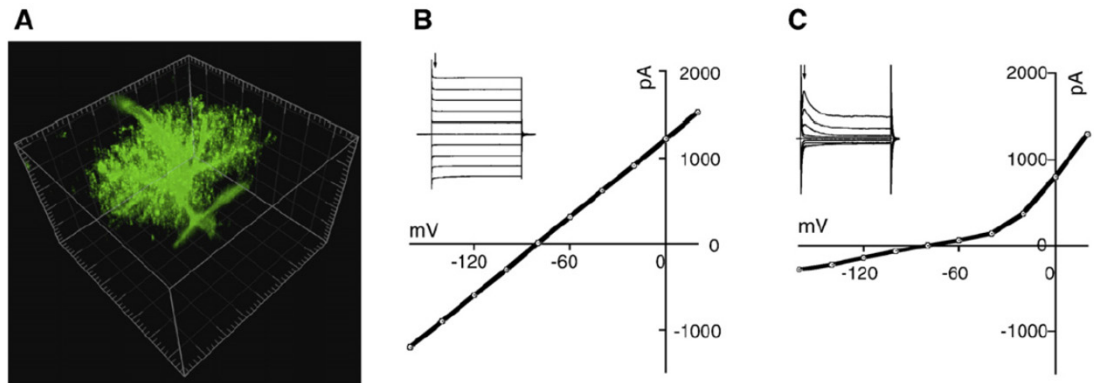


Figure 1



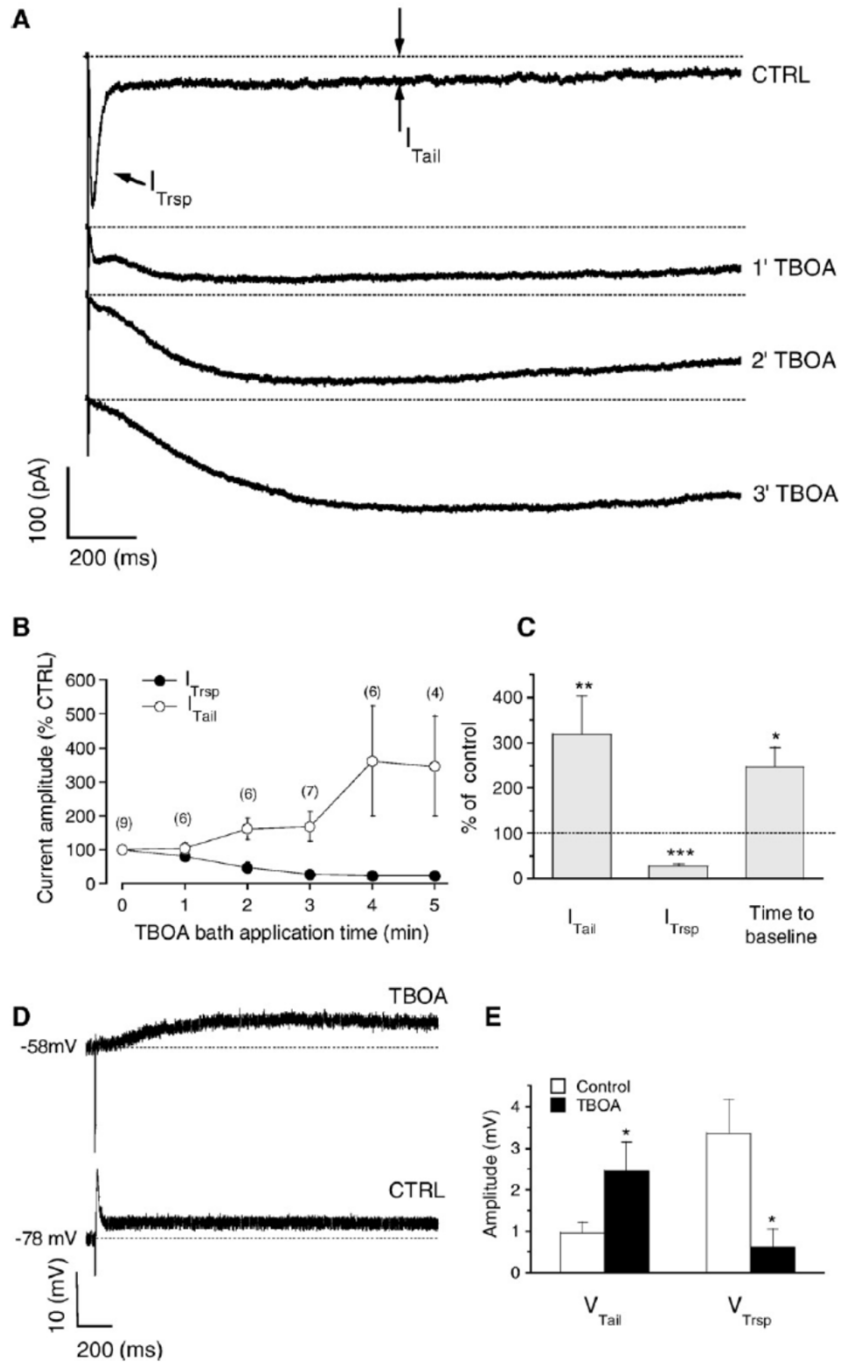


Figure 2

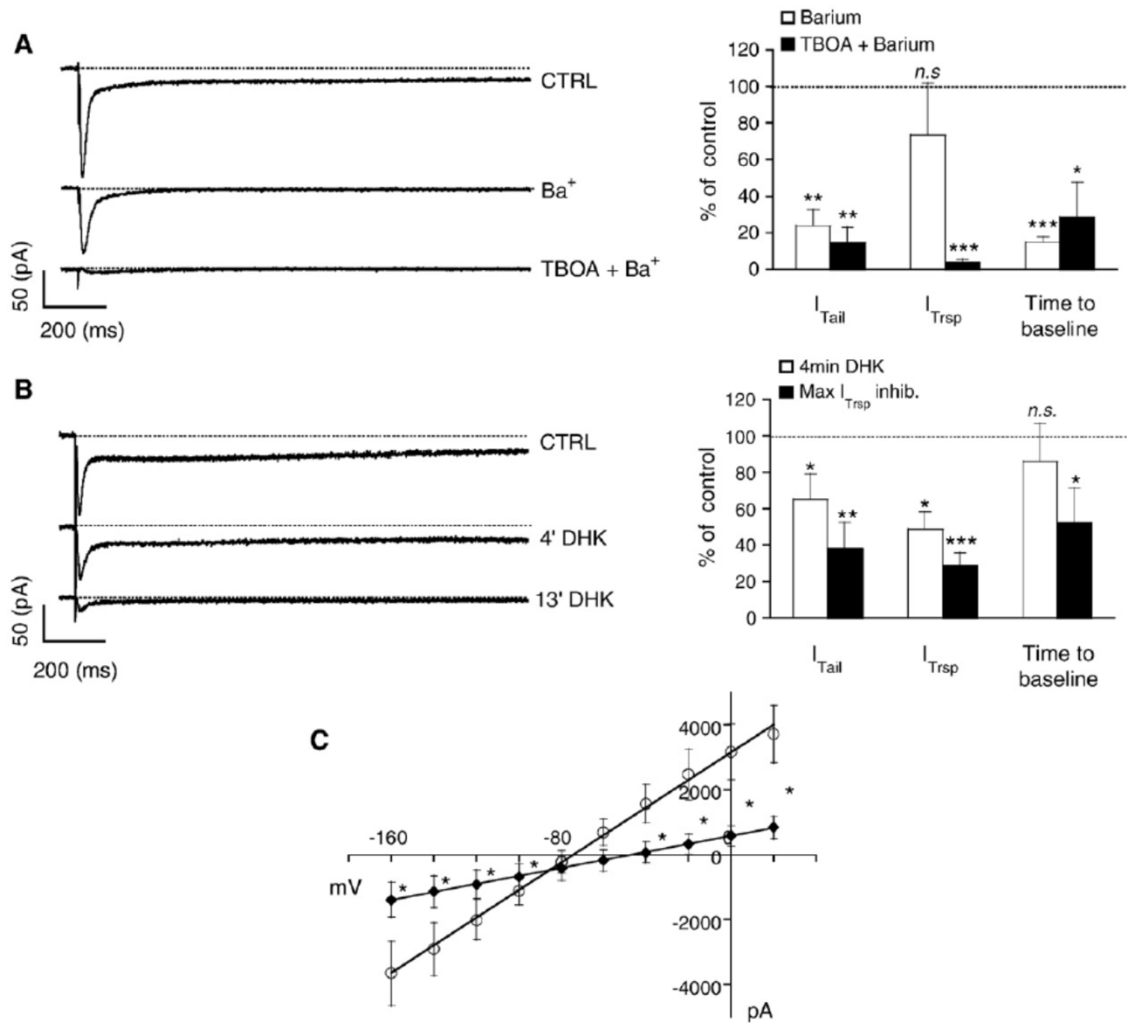


Figure 3